RAPID COMMUNICATIONS

PHYSICAL REVIEW A VOLUME 44, NUMBER 2 15 JULY 1991

Time-resolved study of hot dense germanium by L-shell absorption spectroscopy

J. Bruneau, A. Decoster, D. Desenne, H. Dumont, J.-P. Le Breton, M. Boivineau, J.-P. Perrine, S. Bayle, and M. Louis-Jacquet
Centre d'Etudes de Limeil-Valenton, 94195 Villeneuve Saint Georges, France

J.-P. Geindre, C. Chenais-Popovics, and J.-C. Gauthier
Laboratoire de Physique des Milieux Ionisés, Ecole Polytechnique, 91128 Palaiseau, France
(Received 25 March 1991)

We have used time-resolved $2p$-$3d$ absorption spectroscopy to probe the ionization degree of a germanium plasma heated by the soft x rays emitted from the rear side of laser-irradiated gold targets. We have determined the average ionization degree and the distribution of ion stages as a function of time during the expanding, cooling phase of the plasma. They have been compared with collisional-radiative distributions based on hydrodynamic simulations of the plasma parameters. Results show a slow decrease of the ionization degree from $\langle Z\rangle = 11.5$ to 10.0 during a 3-ns period after gold heating. Comparison with theoretical spectra show matter densities around 0.01 g/cm^3 and temperatures of about 50 eV.

In a previous Letter [1] (from now on referred to as I) we have demonstrated the usefulness of L-shell absorption spectroscopy to probe the electron temperature of medium-Z laser-produced plasmas. A high-Z material layer, directly heated by the driving laser, was deposited on a sample layer of germanium ($Z=32$) in which plasma conditions were probed by absorption measurements of the front layer radiation. We observed the time evolution of the distribution of the ion stages. The average ionization increases sharply during the rising edge of the laser pulse, stays constant during the laser pulse and then decreases with a characteristic time constant of 1.5 ns, i.e., about ten times the laser decay time.

The drawback in this target arrangement is that the laser-irradiated front layer acts both as the heating source and the backlighter source. This does not allow one to study the plasma evolution of the sample layer after the end of the driving laser pulse. The use of a separate backlighter [2] partly solves the problem. Yet, the need of a laser-irradiated heating layer remains. In both experimental schemes, the hydrodynamic mixing occurring at interfaces between the light material and the heavy material plasmas can complicate the interpretation of the absorption measurements [3].

To improve the experimental situation, we have designed a target in which the heating and probing functions are separated [4]. It is made of a thin sample of germanium of 180 $\mu g/cm^2$ areal density tamped by two 150-nm plastic (CH) layers. Four laser-irradiated gold foils of 250 $\mu g/cm^2$ areal density provide the heating radiation (see Fig. 1). The x rays emitted from the rear of the gold foils heat the sample, which is probed by the absorption of a praseodymium backlighter produced by an auxiliary time-delayed laser beam. As the sample is irradiated by x rays on both sides, we can expect to obtain a plasma with much shallower electron-density gradients than in multilayered targets with a direct laser drive.

The experiments were performed using the Octal Nd:glass laser facility at the Centre d'Etudes de Limeil-Valenton. The eight main beams smoothed by random-phase plates were grouped by pairs, each pair being focused on a gold foil. The total energy was about 350 J at the wavelength of 0.35 μm in a 1-ns flat pulse. Under these conditions, the irradiance on the gold foils was 2×10^{14} W/cm^2. The diagnostic beam of Octal (1.053-μm pulse containing 35 J in 400 ps) was focused on a praseodymium target with an adjustable time delay of up to 4 ns with respect to the main beams. The distance between the backlighter and the target was 20 mm. The beam axes were tilted so that the sample could not be heated directly even if the laser had burned through the gold foil before the end of the laser pulse.

Spectra were obtained by two identical spectrographs using 400-mm-diam curved thallium acid phthalate (TlAP) crystals and registered on Kodak SB2 films. The first spectrograph was aligned on the backlighter to sample axis (SP1 in Fig. 1). It allowed the observation of the praseodymium spectrum absorbed by the germanium

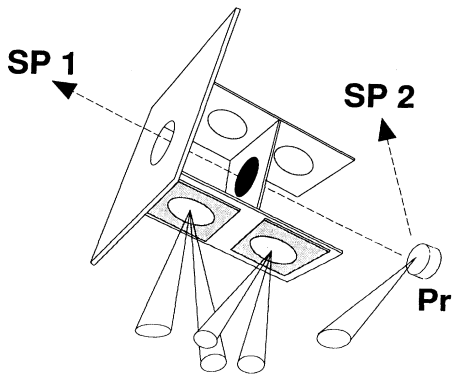

FIG. 1. Target and experimental geometry. Two laser beams are focused on each gold foil (only 4 beams are drawn), the diagnostic beam is focused on the Pr backlighter. Au and Ge foils have a diameter of 600 μm. SP1 and SP2 arrows indicate the direction of observation of the two spectrographs. The distance between two opposite gold foils is 800 μm.

plasma. The second spectrograph was off axis and recorded only the praseodymium spectrum. The comparison of these two spectra for each shot was used to deduce the optical depth of the sample.

Under these experimental conditions, the measured total rear side x-ray emission was about 20% of the incoming laser energy [5,6]. Including geometrical effects due to the limited solid angle over which the heating radiation reached the germanium layer (see Fig. 1), we can assume that about 6–8 J of x rays were effectively used to heat the sample. This is a factor of 2 less than in the multilayered target arrangement used previously. This leads to temperatures lower than the 100 eV quoted in I. Instead of populating the isoelectronic sequences between the Al-like and Ar-like ions, we expect to populate ions from Ca-like to Fe-like, which absorb radiation in the 9.5–10.5 Å range.

Figure 2 shows the optical depth of a germanium plasma as a function of wavelength at two different times. In Figs. 2(a) and 2(b), we have plotted the results obtained at the center of the driving laser pulse and 3 ns later, respectively. The $2p$-$3d$ transitions from ions around the Ti-like sequence provide the unresolved structure that lies between 9.6 and 10.3 Å. From Figs. 2(a) to Fig. 2(b), this structure is shifted toward longer wavelengths by 0.1 Å. This is an effect of the cooling and thus of the recombination of the plasma which is less ionized at later times.

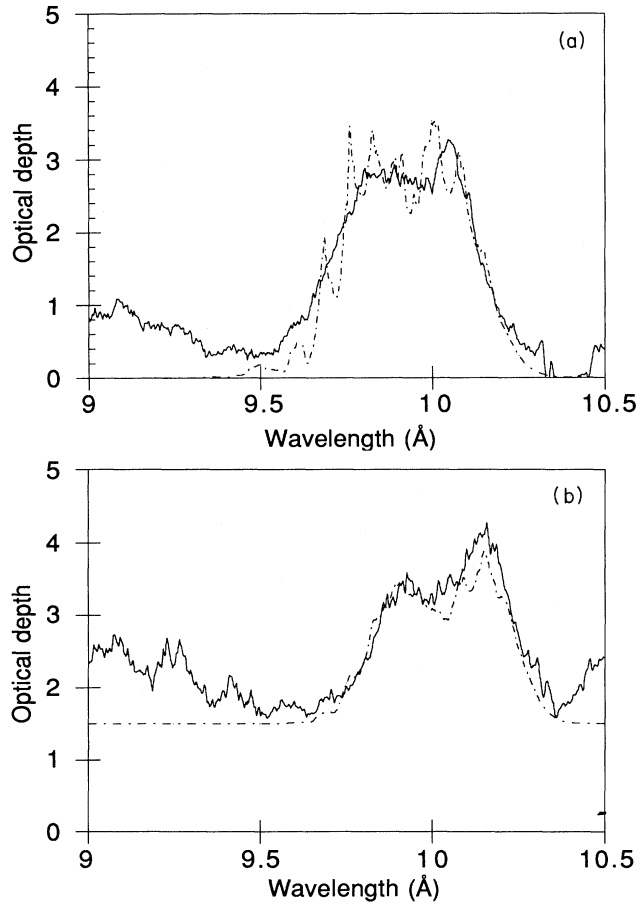

FIG. 2. Optical depth of germanium as a function of wavelength. Solid line: experimental spectrum; dashed line: calculated spectrum at (a) the maximum of the laser pulse and (b) 3 ns later.

The simulation of the optical depth spectra shown in Fig. 2 was carried out with the help of three different numerical tools. The density and temperature of the germanium plasma were inferred from hydrodynamic simulations using the measured laser parameters and the target shape. The distribution of the ionic species prevailing under these plasma conditions was calculated by a collisional-radiative model. The wavelengths and oscillator strengths of these ions were determined by a detailed atomic physics code.

The plasma simulations have been performed with the plane, one-dimensional code CHIVAS-T [7], which solves Lagrangian hydrodynamics together with multigroup radiation diffusion and nonlocal-thermodynamic-equilibrium (average-ion model) atomic physics. The spectrum of the radiation emerging from the rear of the gold heating foil was first calculated as a function of time using the measured irradiance of the laser drive beams. A reduction factor was applied to the x-ray heating flux to take into account the target geometry. In a second simulation, the germanium sample tamped by CH was irradiated by the previously calculated time-dependent x-ray spectrum from the gold plasmas. Results show that after a delay of 1 ns with respect to the center of the laser pulse, the electron density gradient becomes very shallow. Typically, the electron density varies by a factor of 2 from the center to the edge of the foil. The electron temperature is constant over the whole extent of the germanium layer with only a slight decrease of a few electron volts near the edge. Over a 4 ns period starting at the center of the laser pulse, electron densities at the foil center decrease from 2×10^{21} to 3×10^{20} cm^{-3} and electron temperatures from 75 to 40 eV (see Fig. 3).

The ion stage distribution is calculated by a postprocessor that includes a steady-state, detailed-configuration

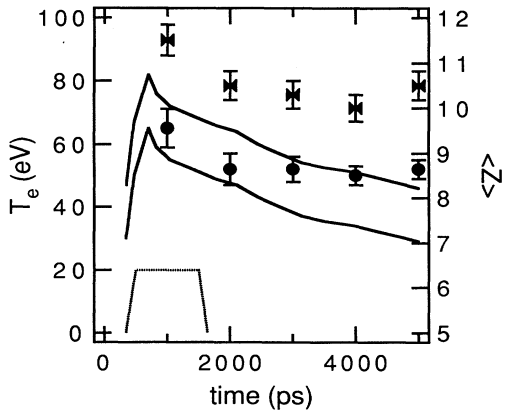

FIG. 3. Variation of the average ionization and of the electron temperature as a function of time. Triangles, measured ionization degree; circles, measured temperatures; and solid line, temperature results from the hydrocode showing the effect of varying by ± 50% the geometrical coupling coefficient. Dotted line is laser pulse shape.

collisional-radiative model (CR). The steady-state approximation is justified because the hydrodynamic time scale, as determined by the hydrocode simulations, is very much larger than the excitation or ionization time scale under our plasma conditions. In this model, energy levels, radiative rates, and excitation and ionization rates are calculated from a screened hydrogenic model.

The optical depth spectrum of the $2p$-$3d$ transitions is generated by a multiconfiguration Dirac-Fock (MCDF) code [8] that calculates the wavelengths and the oscillator strengths for all the relevant ionization stages. We have restricted our calculations to the low-lying manifold of ground states. This approximation, which has also been used in I, can be safely made since the temperature is low and the population of configurations with vacancies in both the $3d$ and the $3p$ or $3s$ subshells is expected to be negligible [9].

A direct comparison between the theoretical and the measured optical depth spectra does not allow to determine independently the temperature and the density of the sample layer [2]. A fitting procedure involving two steps was used. First, the shape of the experimental spectrum was compared with simulations combining the CR ion distributions and the MCDF atomic data at a given average ionization degree to give the best fit for the lower and upper wavelength limits at half maximum of the absorption structure. We found that it was possible, for a given average ionization, to obtain a good agreement for both limits. The second step consisted in adjusting the areal density to reproduce the absolute value of the experimental optical depth. The values used were 130 and 90 $\mu g/cm^2$ for times 0 and 3 ns, respectively.

Results of the comparison are shown in Fig. 2. The average ionization degree giving the best fit in Fig. 2(a) is $\langle Z\rangle = 11.5 \pm 0.3$, and in Fig. 2(b) is $\langle Z\rangle = 10.0 \pm 0.3$. In Fig. 2(a), only 4 species around the Ca-like ions and in Fig. 2(b), only 3 species around the Ti-like ion have relative populations above 10%. As a result, the two spin-orbit components of the transitions $2p_{1/2}$-$3d_{3/2}$ and $2p_{3/2}$-$3d_{5/2}$ are clearly separated in Fig. 2(b). This is good confirmation that the plasma conditions are homogeneous in the germanium layer. Complete results for the variation of the average ionization degree as a function of time are given in Fig. 3.

At several times during and after the driving laser pulse, we have determined the electron temperature by comparing the measured ionization degree to the CR ionization degree using the calculated hydrocode density. Results are shown in Fig. 3 and compared to the electron temperature directly obtained from the hydrocode. In the calculations, the center of the laser pulse was positioned at 1 ns; this corresponds to the time origin for the measurements where the maximum of the backlighter pulse was centered on the main laser pulse. The two solid curves show the effect of varying the geometrical coupling coefficient by $\pm 50\%$ on the germanium temperature. A good agreement between theory and experiment is found up to 2 ns. At later times, the measured average ionization degree increases slightly and the measured electron temperature remains constant, instead of decreasing due to plasma expansion.

The most striking result in this experiment is the steadiness of the electron temperature and of the ionization degree after 3 ns. Postprocessing the CHIVAS-T plasma parameters with the CR model give a variation of the average ionization degree from $\langle Z\rangle = 12.5$ at 1 ns to $\langle Z\rangle = 9$ at 5 ns. The time variation of the electron density can be much faster in the experiment due to lateral expansion effects. Since the decrease of temperature and density has inverse effects on the average ionization, this could introduce a compensating factor in the ionization-degree time evolution. In the CHIVAS-T simulations, the gold plasma x-ray intensity also can be underestimated at late times due to unforeseen radiation confinement effects by the two opposite gold plasmas [10].

In Fig. 2(b), we notice an important continuous absorption corresponding to an optical depth of about 1.5. We suggest that this structure-free absorption arises from the expanding gold plasmas that partially obstruct the space between the two opposite heating gold foils. From 0 to 4 ns, the germanium plasma expands almost linearly with time over a distance of 450 μm. This corresponds to an expansion velocity of about 10^7 cm/s. A collision between the two plasmas can be expected when the germanium sample expands more than 300 μm from its original position. This occurs at 1.8 ns after laser maximum ($t = 2.8$ ns in Fig. 3), which corresponds exactly to the onset of the spurious continuous absorption in the measurements [see Fig. 2(b)]. If the interaction between germanium and gold plasmas is collision dominated [11], the exchange of momentum transfer during the collision blocks the germanium expansion and most of the germanium kinetic energy is converted to thermal energy.

Regarding the areal density problem, the comparison between theory and experiment in Fig. 2 shows that the initial areal density of 180 $\mu g/cm^2$ must be reduced as a function of time to bring theory and experiment into agreement. Since the optical depth depends not only on the areal density but also on the accuracy of the atomic data, we have examined other possible explanations. Oscillator strength errors can be safely ruled out since MCDF calculations are generally accurate to within 10%–20% for strong lines. Saturation of the absorption is negligible in the present case where the overlap between individual lines is very large [12]. We tentatively attribute this density reduction to lateral expansion effects not incorporated in our one-dimensional analysis.

In conclusion, we have measured the time evolution of the ionization degree and the electron temperature in a germanium sample radiatively heated by the x-ray emission of a high-Z secondary plasma. The resulting germanium plasma exhibits densities and temperatures, that are by far more homogeneous than in conventional laser-irradiated multilayer target experiments. However, our measurements are perturbed at late times by the collision of the radiatively-heated sample plasma and the heating plasmas. In addition, lateral expansion of the heated foil reduces its areal density. The hydrodynamic simulation correctly describes the evolution of the temperature over a 2 ns period following the maximum of the x-ray driving pulse. Our simple one-dimensional analysis of plasma expansion is probably inadequate at late times. We would

like to point out that the present technique can be used in x-ray laser research. Our results clearly show that the range of plasma parameters which can be resolved in time by absorption measurements of a separate backlighter source covers the range that is useful to understand the kinetics of x-ray lasers using the recombination pumping scheme [13,14].

We would like to thank J-M. Koenig, L. Lance, J.-L. Larcade, B. Pupille, M. Rabec le Gloahec, and J. Turberville for the help on the Heliotrope target chamber, the Octal laser team for technical assistance, and acknowledge the very efficient and skillful work of H. Arrignon, M. Bellingard, and R. Caland for target preparation.

[1] J. Bruneau, C. Chenais-Popovics, D. Desenne, J.-C. Gauthier, J.-P. Geindre, M. Klapisch, J.-P. Le Breton, M. Louis-Jacquet, D. Naccache, and J.-P. Perrine, Phys. Rev. Lett. **65**, 1435 (1990).

[2] J. P. Geindre, C. Chenais-Popovics, P. Audebert, C. A. Back, J. C. Gauthier, H. Pepin, and M. Chaker, Phys. Rev. A **43**, 3202 (1991).

[3] J. C. V. Hansom, P. A. Rosen, T. J. Goldsack, K. Oades, P. Fieldhouse, N. Cowperthwaite, D. L. Youngs, N. Mawhinney, and A. J. Baxter (unpublished); J. Kilkenny, Phys. Fluids B **2**, 1400 (1990).

[4] S. J. Davidson, J. M. Foster, C. C. Smith, K. A. Warburton, and S. Rose, Appl. Phys. Lett. **52**, 847 (1988).

[5] K. Kondo, H. Nishimura, K. Kongo, H. Hasegawa, Y. Kato, T. Yamanaka, S. Nakai, and K. Taniguchi, J. Appl. Phys. **67**, 2693 (1990).

[6] D. Babonneau, J. L. Bocher, C. Bayer, A. Decoster, D. Juraszek, X. Fortin, J. P. Perrine, and G. Thiell (unpublished).

[7] A. Decoster (unpublished).

[8] J. Bruneau, J. Phys. B **17**, 3009 (1984).

[9] J. C. Gauthier, J. P. Geindre, C. Chenais-Popovics, M. Louis-Jacquet, J. Bruneau, D. Desenne, D. Naccache, C. Bauche-Arnoult, and J. Bauche, in *International Workshop on Radiative Properties of Hot and Dense Matter,* edited by W. Goldstein, R. Lee, C. Hooper, S. Rose, and J. C. Gauthier (World Scientific, Singapore, 1991).

[10] G. D. Tsakiris *et al.*, Phys. Rev. A **42**, 6188 (1990).

[11] F. Glas and M. Schnürer (private communication).

[12] C. Chenais-Popovics, C. Fievet, J. P. Geindre, I. Matsushima, and J. C. Gauthier, Phys. Rev. A **42**, 4788 (1990).

[13] R. C. Elton, *X-Ray Lasers* (Academic, New York, 1990), and references herein.

[14] A. Carillon *et al.*, J. Phys. B **23**, 147 (1990).